# Challenges in flood modeling over data scarce regions: how to exploit globally available soil moisture products to estimate antecedent soil wetness conditions in Morocco

El Mahdi El Khalki [1], Yves Tramblay[2,*], Christian Massari[3], Luca Brocca[3], Vincent Simmoneaux[4], Simon Gascoin[4], Mohamed El Mehdi Saidi[1]

[1] Georesources, Geoenvironment and Civil Engineering Laboratory, Cadi Ayyad University, Marrakesh, 40000, Morocco

[2] HydroSciences Montpellier (Univ. Montpellier, CNRS, IRD), Montpellier, 34000, France

[3] Research Institute for Geo-Hydrological Protection, National Research Council, Perugia, 06100, Italy

[4] Centre d'Etudes Spatiales de la Biosphère (UPS/CNRS/IRD/CNES), Toulouse, France

* Correspondence to: Yves Tramblay (yves.tramblay@ird.fr)

**Abstract:** The Mediterranean region is characterized by intense rainfall events giving rise to devastating floods. In Maghreb countries such as Morocco, there is a strong need for forecasting systems to reduce the impacts of floods. The development of such a system in the case of ungauged catchments is complicated but remote sensing products could overcome the lack of in-situ measurements. The soil moisture content can strongly modulate the magnitude of flood events and consequently is a crucial parameter to take into account for flood modeling. In this study, different soil moisture products (ESA-CCI, SMOS, SMOS-IC, ASCAT satellite products and ERA5 reanalysis) are compared to in-situ measurements and one continuous soil moisture accounting (SMA) model for basins located in the High-Atlas Mountains, upstream of the city of Marrakech. The results show that the SMOS-IC satellite product and the ERA5 reanalysis are best correlated with observed soil moisture and with the SMA model outputs. The different soil moisture datasets were also compared to estimate the initial soil moisture condition for an event-based hydrological model based on the Soil Conservation Service Curve Number (SCS-CN). The ASCAT, SMOS-IC and ERA5 products performed equally well in validation to simulate floods, outperforming daily in situ soil moisture measurements that may not be representative of the whole catchment soil moisture conditions. The results also indicated that the daily time step may not fully represent the saturation state before a flood event, due to the rapid decay of soil moisture after rainfall in these semi-arid environments. Indeed, at the hourly time step, ERA5 and in-situ measurements were found to better represent the initial soil moisture conditions of the SCS-CN model by comparison with the daily time step. The results of this work could be used to implement efficient flood modelling and forecasting systems in semi-arid regions where soil moisture measurements are lacking.

**Keywords:** Soil moisture, floods, Morocco, ERA5, Rheraya, Issyl, High Atlas

**1 Introduction**

The Mediterranean region is characterized by intense rainfall events generating floods with a very short response time (Gaume et al., 2004; Merheb et al., 2016; Tramblay et al., 2011). The socio-economic consequences of these floods are very important in terms of fatalities or damages to the infrastructures in particular for Southern countries (Vinet et al., 2016). This highlights the need for forecasting systems to reduce the impacts of floods. Unfortunately, the development of such systems is very complicated in the case of ungauged catchments (Creutin and Borga, 2003) such as in North Africa and requires remote sensing products to overcome the lack of in situ measurements. Furthermore, while several studies have been focused on northern Mediterranean catchments for flood modelling, only a few studies are available on southern basins, yet those probably the most vulnerable to floods.

The Moroccan catchments are exposed to intense flash floods, such as the event of August 17, 1995 in the Ourika river where the max discharge reached in 45 minutes a peak discharge of 1030 m3/s causing extensive damages and more than 200 casualties (Saidi et al., 2003). Few studies have been carried out in Morocco to minimize the impact of floods by improving the forecasting systems, either by event-based modeling of floods (El Alaoui El Fels et al., 2017; Boumenni et al., 2017; El Khalki et al., 2018) or by hydro-geomorphological approaches (Bennani et al., 2019) to identify the areas at risk of flooding. The severity of floods in these semi-arid regions is controlled by several factors including precipitation intensity, soil permeability, steep slopes and soil moisture content at the beginning of event (El Khalki et al., 2018; Tramblay et al., 2012). In Mediterranean regions, the soil moisture content varies between events and is known to strongly modulate the magnitude of floods (Brocca et al., 2017; Tuttle and Salvucci, 2014) and particularly to be useful for flood modeling and forecasting systems (Brocca et al., 2011; El Khalki et al., 2018; Koster et al., 2009; Marchandise and Viel, 2010; Tramblay et al., 2012). However, studies in North African basins are lacking to document the rainfall-runoff relationship with soil moisture during floods (Merheb et al., 2016).

In most Mediterranean regions and particularly in North Africa, only a few measurements of soil moisture are available. To represent spatial variability, several measurement at different locations are needed due to the potentially large spatial variability of soil moisture for a wide range of scales (Massari et al., 2014; Schulte et al., 2005; Western and Blöschl, 1999). However, even the in-situ data may not represent the spatial variability over a very wide area in the case of large basins. On the contrary, satellite soil moisture products provide coverage of the earth's surface by microwave sensors. There are two types of microwave sensors, active and passive, noting: 1) The Advanced Scatterometer (ASCAT) soil moisture product is on board MetOp with good radiometric accuracy and stability. This product provides

a spatial resolution of 25 km with a temporal resolution of 1 day since January 2007 (Wagner et al., 2013). 2) The Soil Moisture and Ocean Salinity Mission (SMOS) product, which begins in January 2010 with a spatial resolution of 50km (Kerr et al., 2012). The improvement of the robustness of satellite soil moisture products can be achieved by merging passive and active microwave sensors as initiated and distributed by ESA-CCI (European Space Agency Climate Change Initiative) (Liu et al., 2011) providing data from 1978 to 2018. However, remote sensing products might suffer from several problems in complex topography or very dense vegetation and snow cover (Brocca et al., 2017). For this reason and before any use the data, it is necessary to validate them (Al-Yaari et al., 2014; Van doninck et al., 2012; Ochsner et al., 2013), either by in-situ measurements, if they exist, or by using Soil Moisture Accounting models (Javelle et al., 2010; Tramblay et al., 2012) to simulate soil moisture in the ungauged basins.

In this context, with an increasing number of satellite products becoming available to estimate soil moisture, clear guidelines and recommendations about the most suitable products to estimate the initial soil moisture content prior to floods are lacking for the semi-arid basins of North Africa. There is a knowledge gap on the evaluation of soil moisture products in North Africa (Jiang and Wang, 2019) that the present study aimed to fill. The purpose of this study is to compare different satellite soil moisture products with in-situ soil moisture measurements and the recently developed ERA5 reanalysis to estimate the initial soil moisture before flood events. The goal is to identify the best products to be used for flood modeling that could improve forecasting systems. This comparison is performed for two basins representative of medium-size catchments of North Africa that are the most sensitive to flash flood events. The validation of the different soil moisture products is made with a Soil Moisture Accounting (SMA) model, to test the capabilities of the different soil moisture products for the sake of estimating the initial conditions for an event-based hydrological model for floods. The paper is organized as follow: In section 2, an overview of the study area and all used data (hydro-meteorological and soil moisture products). Section 3 explains the methods adopted in this paper. Section 4 presents the results. The conclusion and perspectives are given in the last section.

**2 Study area and data**

**2.1 Rheraya and Issyl catchments**

The Rheraya research catchment (Jarlan et al., 2015) is located in the Moroccan High Atlas Mountains (Figure 1) with an altitude ranging from 1027 to 4167m and an area of 225km². The climate in the basin is semi-arid, strongly influenced by altitude, with a mean annual precipitation of 732mm, including 30% as snow in altitudes above 2000m (Boudhar et al., 2009). The geology is characterized by volcanic formations that are considered impermeable in the highest elevation areas, while the lowest elevation

areas are made of granites with clays and marls. In the highest elevation areas very steep slopes are found with an average of 19% (Chaponnière et al., 2008). The vegetation cover is only located in the lowest areas with a concentration of cultivated areas found along the river channel. These natural conditions favor runoff generation. There is very low human disturbance for runoff, with only some local water uptake in the lower part of the river.

The Issyl basin (Figure 1) is located in the foothills of the Moroccan High Atlas Mountains with an altitude ranging from 632 to 2300m, an area of 160 km², and a mean annual precipitation of 666mm. It is an ephemeral river with discharge occurring only after rainfall events. The climate is semi-arid to arid and the downstream part of the basin reaches the city of Marrakech. The geological formations in this downstream are alluvial conglomerates that are relatively permeable. The upstream of the basin consists of clays and calcareous marl. The basin area includes agricultural activities that are irrigated in the downstream part of the basin. The irrigation comes from *seguias*, earthen-made channels that traditionally draw their water supply from the river itself, by building small diverting dams on the side of the river (Pérennès, 1994). The *seguias* channels are usually filled up during floods, and water is distributed to the neighboring agricultural parcels. The map on the *seguias* in the Issyl basin can be seen in Figure 1, covering the northern part of the basin. The system is unmonitored and in a context of high evaporation rates the portion of runoff diverted from the stream is not quantified. Due to the temporary nature of *seguias*, they can be partially destroyed during large floods and consequently their hydraulic properties and the amount of water collected can be modified over time. In the Ourika catchment located upstream of the Issyl, Bouimouass et al. (2020) estimated that irrigation by streamflow diversion due to *seguias* could represent up to 65% of the total surface runoff.

**2.2 Hydro-meteorological data**

In the Rheraya basin, we used 8 rainfall stations (Table 1), 5 of them from the data network of the Joint International Laboratory Télédétection et Ressources en Eau en Méditerranée semi- Aride ''LMI TREMA'' (Jarlan et al., 2015; Khabba et al., 2013) and the remaining ones from the Tensift Hydraulic Basin Agency. The data is covering from 2008 to 2016. For the Issyl basin, only 2 rainfall gauges are available from the Tensift Hydraulic Basin Agency, covering the years from 2010 to 2015. In this type of basin, the spatial variability of rainfall is very important (Chaponnière et al., 2008). The hydrometric data was provided by radar sensor installed in each basin's outlet. The data is covering only the year 2014 for Rheraya, since the sensor was installed at the end of 2013, and the years 2010 to 2015 for Issyl. The discharge data is provided with a time step of 10min converted into hourly time step as for rainfall.

The precipitation data is missing for some events, especially at at high altitude gauges during snowfall events. The percentage of missing value ranges from 2.4% at PR5 to 10.85% at PR7. The highest

149    percentage of missing data is 19.7% at PR1 where the gauge underwent technical problems. Overall,

150    the total percentage of missing value (7.8%) is low, hence and no gap filling method is used. The

151    discharge data is missing in some events that are not selected. For this reason we considered only the

152    events with complete discharge data. Some of the flood events considered in this study (Table 2)

153    occurred in winter season, where rainfall can be in the form of snow above 2000m elevation. According

154    to El Khalki et al.(2018), the snow does not contribute to runoff during winter season in the Rheraya

155    basin because it does not melt during the coldest months (Hajhouji et al., 2018), where only 17% of

156    basin area is occupied by snow. The runoff coefficient is calculated by relating the amount of direct

157    runoff to the amount of precipitation for each selected events. It is larger when the basin has low

158    infiltration and lower for permeable basins. In our case, runoff coefficient ranges from 13.1 to 34.1%

159    for Rheraya and from 1.2 to 7.2% for Issyl. This indicates the important role of initial conditions in both

160    basins, with a much higher infiltration capacity in the Issyl basin in addition to potential water loss due

161    to irrigation. We used 5 temperature stations located in the Rheraya basin and one temperature station

162    located in the Issyl basin with an hourly time step to calculate the average temperature over each basin,

163    ranging from 2008 to 2016. This data enabled us to calculate potential evapotranspiration (PET) with

164    Oudin formula (Oudin et al., 2005) requiring temperature only. This formula was previously applied in

165    Morocco ((Marchane et al., 2017; Tramblay et al., 2013) and in Tunisia (Dakhlaoui et al., 2020).

166

167    **2.3 Soil moisture data**

168

169    We used 7 different types of soil moisture data over the Rheraya basin and 6 types in the Issyl basin due

170    to the absence of measurements in this basin. Covering the same period of rainfall data mentioned in the

171    2.3 section, we used:

172              1. In-situ measurement with three Thetaprobes at 5cm and 30cm depth in the Rheraya basin,

173                 located at the SMPR7 station (Figure 1).

174              2. Simulated soil moisture from a Soil Moisture Accounting model (SMA)

175              3. ASCAT satellite soil moisture

176              4. SMOS satellite soil moisture

177              5. SMOS-IC satellite soil moisture

178              6. ESA-CCI satellite soil moisture

179              7. ERA5 reanalysis soil moisture

180

181    **2.3.1 In-situ measurements**

182

183    Soil moisture measurements are available at one location with three Thetaprobes at two different depths

184    (5cm and 30cm). In this study we used Thetaprobes with 5cm depth, which is comparable with the

185    depths of satellite products (Massari et al., 2014). The site is located in Rheraya basin, with an altitude

of 2030m and a slope of 30% (Figure 1). The data is covering the time period from 2013 to 2016, with 30min time step converted to daily time step.

**2.3.2 Soil moisture accounting model**

The SMA is a continuous Soil Moisture Accounting model that can be used in the absence of soil moisture data to represent the degree of saturation for flood modeling (Anctil et al., 2004; Tramblay et al., 2012). In this study, a simplified version of the SMA model is used, adopting the same approach used by Tramblay et al. (2012) and Javelle et al. (2010). The SMA calculates the level of the soil reservoir (S/A), ranging between 0 and 1, by calibrating its single parameter, A, which represents the maximum reservoir capacity of the soil. An interpolated daily rainfall dataset created by the Inverse Distance method and evapotranspiration data computed from daily temperature with the Oudin equation (Oudin et al., 2005) are used as inputs to the SMA model.

**2.3.3 Soil moisture products**

In this study we used three different types of satellite products and a Reanalysis product (Table 3):

1. The Advanced SCATterometer (ASCAT) is a Soil Moisture product, onboard Metop-A and Metop-B and a Metop-C satellite is a C-band (5.255 GHz) scatterometer onboard the Metop satellite series. It has a spatial sampling of 12.5 km and 1 to 2 observations per day (Wagner et al., 2013). The SM product was provided within the EUMETSAT project (http://hsaf.meteoam.it/) denoted as H115.

2. The Soil Moisture and Ocean Salinity (SMOS) mission is a radiometer operating at L band (1.4 GHz), providing Soil Moisture data with ~50km as spatial sampling and 1 observation per 2/3 days (Kerr et al., 2001). Centre Aval de Traitement des Données SMOS (CATDS, https://www.catds.fr/) provided the version RE04 (level3) for this study. This version is gridded on the 25km EASEv2 grid.

3. The Soil Moisture and Ocean Salinity INRA-CESBIO (SMOS-IC) is an algorithm designed by Insitut National de la Recherche Agronomique (INRA) and Centre d'Etudes Spatiales de la Biosphère (CESBIO) for a global retrieval of Soil Moisture and L-VOD. Two parameters of inversion of the L-MED model are used in the SMOS-IC (Wigneron et al., 2007) with a consideration of the pixel as homogeneous. This version is 105 and has a spatial sampling of 25km with EASEv2 grid (Fernandez-Moran et al., 2017).

4. The ESA-CCI soil moisture product (http://www.esa-soilmoisture-cci.org/) regroups active and passive microwave sensors to measure soil moisture, giving three type of products: Active, Passive and Combined (Active + Passive). In this paper, the ESA-CCI V4.5 –

223              Combined product is used (Dorigo et al., 2017; Gruber et al., 2017, 2019). The product has

224              been  validated to be useful by 600 ground-based measurement points around the globe

225              (Dorigo et al., 2015), as well as it was compared with ERA-Interim products (Albergel et

226              al., 2013). In the field of hydrological modeling, several global studies have used the ESA-

227              CCI product to initiate the hydrological model (Dorigo et al., 2012, 2015; Massari et al.,

228              2014) at the scale of Morocco (El Khalki et al., 2018). We extracted for each basin the

229              pixel that corresponds to it.

230       5.  ERA5 (Copernicus Climate Change Service (C3S), 2017) developed by European Centre

231              for Medium-Range Weather Forecasts (ECMWF), it is the latest version of atmospheric

232              reanalysis available for public since February 2019. The ERA5 replaced ERA-Interim with

233              improvement at different scales, particularly, a higher spatial and temporal resolution, and

234              a better global balance of precipitation and evaporation. The spatial resolution is 31km

235              instead of 79km, hourly resolution is used instead of 6 hours, and the covered period will

236              be extended to 1950 in future. The ERA5 product was applied in some recent studies in

237              hydro-climatic field (Albergel et al., 2018; Hwang et al., 2019; Mahto and Mishra, 2019;

238              Olauson, 2018). We selected the volumetric soil water of the first soil layer. This new

239              product is tested in our study for the first time in Morocco. An alternative dataset, ERA5-

240              Land using an improved land-surface scheme with a spatial resolution of 10km, was also

241              tested, providing the same results as ERA5 since there is a strong correlation between soil

242              moisture simulated by the two products.

243

244    It should be noted that the soil moisture products have a different percentage of missing data over each

245    basin (Table 4). The ESA-CCI product  show an important percentage of missing values over the

246    Rheraya basin compared to ASCAT that is included in the ESA-CCI product. This is due to the filter

247    used in the ESA-CCI product to ensure the data quality. The difference in the percentage of missing

248    values between Rheraya and Issyl is related to the complex topography and also to the frozen zones in

249    the Rheraya basin, more description about the applied filters can be found in (Dorigo et al., 2017).

250    However, the percentage of missing values for the SMOS product are quite similar between the two

251    basins, which is related to the low temporal resolution (1 observation per 2/3 days).

252

253    **3 Methods**

254

255    **3.1 Evaluation of different soil moisture datasets**

256

257    In-situ data preparation consists of averaging the 5cm depth probes in order to get a single value to work

258    with and take into account the plot-scale variability of the measurements. This data is considered as a

259    reference for soil moisture data in the Rheraya basin, so that all the other soil moisture products are

260 compared to it. The different soil moisture products are compared to the observed soil moisture over the

261 entire period and also on a seasonal basis.

262

263 The SMA model is used to represent the soil moisture aggregated at the catchment scale. The rationale

264 behind the use of such model here is that continuous rainfall and temperature series are often available

265 in monitored catchments, unlike soil moisture, and a calibrated SMA model can sometimes palliate the

266 lack of soil moisture measurements (Tramblay et al., 2012). For the SMA model, the A parameter,

267 representing the soil water holding capacity, is calibrated to obtain the best correlation between observed

268 and simulated soil moisture (S/A). The calibration with observed data can only be performed in the

269 Rheraya basin where soil moisture is measured. In addition to this calibration, other values of A, ranging

270 from 1 to 1000mm, are tested in the SMA model to maximize the correlations with the different soil

271 moisture products. The choice of this approach is to check if there are any possible uncertainties that

272 can be related to the in-situ soil moisture measurements, located on a steep slope plot that may not fully

273 represent the average soil moisture conditions over the whole basin. In the case of the Issyl basin, since

274 there is no observed soil moisture data, the model is run for a range of different values of the A

275 parameter. The best value of the A parameter is selected as the one yielding the best correlations with

276 the different satellite products.

277

278 The values from ASCAT and SMA are given in percentage (values are ranging between 0 and 1) while

279 SMOS, SMOS-IC, ERA5, ESA-CCI and observations are in $m^3$ $m^{-3}$. To allow a comparison for all soil

280 moisture datasets a rescaling procedure is needed. Before applying the rescaling procedure, according

281 to Albergel et al. (2010), a 95% confidence interval is chosen to define the higher and lower values to

282 exclude any abnormal outliers using equation 1 and 2. The resulted data is then rescaled to their own

283 maximum and minimum values considering the whole period using the equation 3. The issue in the

284 validation of satellite soil moisture products and reanalysis product with in-situ measurements is the

285 spatial resolution (Jackson et al., 2010). Several studies mentioned that, in the case of the temporal

286 stability  introduced by Vachaud et al. (1985), one in-situ measurement point can represent the soil

287 moisture condition of a larger area (Brocca et al., 2009b, 2010; Loew and Mauser, 2008; Loew and

288 Schlenz, 2011; Martínez-Fernández and Ceballos, 2005; Miralles et al., 2010; Wagner et al., 2008).

289 According to (Massari et al., 2015), the coarse satellite observations can be beneficial for small basins,

290 in the case if the in-situ observation falls in the satellite product pixel. This means that the in-situ

291 measurements can represent a good benchmark (Liu et al., 2011). In this study we considered the in-situ

292 measurement as a benchmark to validate different soil moisture products.

293

$$Up_{SM} = \mu_{SM} + 1.96\sigma_{SM}, \tag{1}$$

$$Low_{SM} = \mu_{SM} - 1.96\sigma_{SM}, \tag{2}$$

294

Where $Up_{SM}$ and $Low_{SM}$ are the limits of the confidence interval (the upper and the lower 95%)

$$SM = \frac{SM - Low_{SM}}{Low_{SM} - Up_{SM}}, \tag{3}$$

The correlation coefficient of Pearson equation (4) and the Root Mean Square Deviation (RMSD) equation (5) are used to compare in-situ measurements and humidity modeled by SMA model and the different soil moisture products.

$$r = \frac{N \sum SM_{sat} SM_{In-situ} - (\sum SM_{sat})(\sum SM_{In-situ})}{\sqrt{[N \sum SM_{sat}{}^2 - (\sum SM_{sat})^2][N \sum SM_{In-situ}{}^2 - (\sum SM_{In-situ})^2]}}, \tag{4}$$

$$RMSD = \sqrt{\frac{\sum (SM_{In-situ} - SM_{sat})^2}{N}}, \tag{5}$$

With $SM_{In-situ}$ is the in-situ measurements of soil moisture or SMA model which are considered as reference, $SM_{sat}$ is the soil moisture from satellite or reanalysis and N is the number of values.

**3.2 Event-based hydrological model for floods**

In this study, we used the Soil Conservation Service Curve Number (SCS-CN) model for each basin, implemented in the hydrologic Engineering System - Hydrologic Modeling System ''HEC-HMS'' software (US Army Corps of Engineers, 2015). This model is known by its widespread popularity and to the simplicity of the application method (Miliani et al., 2011). SCS-CN is often used in the semi-arid context (Brocca et al., 2009a; El Khalki et al., 2018; Tramblay et al., 2010; Zema et al., 2017). Our methodology is based on the use of SCS-CN model as a production function to compute net rainfall, by automatically and manually calibrating the Curve Number parameter (CN) in order to obtain a realistic hydrograph shape. The value of CN is non-dimensional ranging from 0 (dry) to 100 (wet). The potential maximum retention, S, is related to CN as follows:

$$S = \frac{25400}{CN} - 254, \tag{6}$$

The transformation of precipitation excess into runoff is provided by Clark Unit hydrograph model (transfer function). The calibration procedure is based on calibrating the Clark Unit hydrograph model parameters; Storage Coefficient (Sc) and Time of Concentration (Tc). The two functions (production and transfer) are calibrated separately to avoid the parameter dependence and the calibration is based on Nash-Sutcliff criterion.

325

The validation procedure is based on two steps; first, testing the relationship between soil moisture data (In-situ, SMA, ERA5, ASCAT, SMOS, SMOS-IC and ESA-CCI), at two different timescales (daily and hourly) and the S parameter of the event-based model of all the flood events. The hourly time step concerns only the in-situ data and ERA5 by choosing the soil moisture state 1 hour before the starting time of rainfall for each event. Only the ERA5 product can be used in the Issyl basin at the hourly time step due to the absence of observed data. Then, the soil moisture products that are well correlated with S parameter are used to validate the model by calculating the S parameter from the linear equation obtained between soil moisture and S, using the leave-one-out resampling procedure; each event is successively removed and a new relationship between the remaining event is re-computed. The relationship is good when the correlation is near to r= -1. The negative correlation is related to the fact that, the storage capacity (S) is larger when the soil is dry (soil moisture is near to 0). The estimated S parameter for a given event is then used in the SCS-CN model in validation. For the Clark Unit Hydrograph model, the average of the Sc and the Tc parameters are used in validation in the leave-one-out resampling method; the parameters are re-calibrated with the remaining events and the mean of calibrated values are used in validation.

341

For the evaluation of the flows simulated by the flood event model, we compared the simulated discharge with those observed using the efficiency coefficient of Nash-Sutcliffe (Ns) (Nash and Sutcliffe, 1970) equation (7) as well as through the bias on peak flow and on volume equation(8).

345

$$Ns = 1 - \frac{\sum((Q_{obs}) - Q_{sim}))^2}{\sum((Q_{obs}) - (\overline{Q_{obs}}))^2}, \tag{7}$$

$$BIAS_Q = \frac{\sum(Q_{sim} - Q_{obs})}{\sum Q_{obs}}, \tag{8}$$

346

Where $Q_{sim}$ is the simulated discharge, $Q_{obs}$ is the observed discharge and n is the number of events The Ns ranges between $-\infty$ and 1, the 1 value of Ns indicates that the simulated discharge perfectly match the observed hydrograph

350

**4 Results and discussions**

352

**4.1 Relationship between satellite soil moisture data and in-situ measurements**

354

The comparison between measured soil moisture at 5cm depth and the different products of soil moisture show that the SMOS-IC and ERA5 provide the best correlations, with r=0.77 and r=0.67 respectively, but it should be noted that all the correlations with the different products are also significant. Figure 2 shows that SMOS-IC and ERA5 reproduce dry periods well, whereas ERA5 reproduces well wet

periods. This result is in accordance with the results of Massari et al. (2014) who found that ERA-Land is well correlated with In-situ data. ASCAT product shows a correlation of r=0.45 which is less than the correlation given in Albergel et al. (2010) who found r values ranging from 0.59 to 0.64, the lower correlation may be caused by the orography and the coarse resolution. In fact, this results shows that the use of a combined product as ESA-CCI give an obvious advances in term of r values than one single satellite soil moisture product (Ma et al., 2019; Zeng et al., 2015).

**4.2 Relationship between the SMA model outputs and soil moisture products**

The best correlation between observed soil moisture and the soil moisture level (S/A) modeled by the SMA model is obtained for A=8mm with r=0.86. But it shows higher RMSD than observations (RMSD =0.23) which is due to the overestimation of the wet periods (Figure 3). This can be related to the averaging of rainfall data in the SMA model over the basin which could be higher than rainfall in the soil moisture measurement site. It should be noted that the value of the A parameter is very small by comparing to previous studies (Javelle et al., 2010; Tramblay et al., 2012), indicating a much lower soil storage capacity.

We correlated the SMA model output (for A=8mm) with the Satellite Products of Soil Moisture, and the best correlations are found for SMOS-IC and ERA-5, with r=0.74 and r=0.63 respectively (Figure 4). Other values of A that maximize the correlations with the different soil moisture products have also been tested. Optimal values of A are ranging from 1 mm with ASCAT (with r= 0.4), 8 mm for SMOS (r=0.56), SMOS-IC (r=0.74) and ESA-CCI (r=0.59) up to 16mm for ERA5 (r=0.68). Comparing the Figure 2 and Figure 4 we notice that the soil moisture products better reproduce in-situ measurements than modeled soil moisture with the SMA model, expect for ESA-CCI and SMOS. This improvement is directly related to the SMA model performance, which overestimates soil moisture, and should be compared to Figure 2 where ESA-CCI and SMOS products also overestimate in-situ measurements.

For the Issyl basin,ss mentioned above, no observed soil moisture data is available to calibrate the A parameter of the SMA model. Therefore, different values of A are tested to correlate the SMA outputs with the different soil moisture datasets. Over all datasets, the value of A best correlated to the majority of soil moisture products is 30mm. The best correlation is given by A=30mm with r=0.78, 0.82 and 0.79 for ASCAT, SMOS-IC and ESA-CCI respectively. As for SMOS and ERA5, the best correlation is given for A=40mm with r=0.7 and A=60mm with r=0.8, respectively. In order to choose a single value of A that represents the basin, we have considered A=30mm, the optimal value yielding the best correlations with the different soil moisture products. Figure 5 shows that the best correlation between satellite products and S/A is obtained with SMOS-IC (r=0.82) and ESA-CCI (r=0.79). As observed over the Rheraya basin, the SMOS-IC and ERA5 products showed a good reproduction for dry periods with

a better reproduction of wet periods with ERA5, these results are similar to those of Ma et al. (2019) who found that SMOS-IC performs well in arid zones with a median r value of 0.6. Overall, the higher value for the A parameter found for this basin is coherent with the fact that this basin is located in a plain area with a much higher soil moisture storage capacity than in the mountainous Rheraya basin.

**4.3. Comparison of soil moisture datasets by seasons**

Seasonal evaluation of satellite soil moisture and reanalysis data shows for the Rheraya basin that during the summer season there are low correlations (average r=0.34) for all the products which is possibly due to very low precipitation amounts mostly as localized convective precipitation (Albergel et al., 2010). On the contrary, better performance are obtained with the SMA model (r=0.59) that considers catchment-scale precipitations. Better correlations are obtained in fall with an average of r=0.61 and 0.58 for the in-situ data and SMA respectively (Table 5). In the winter we found a poor correlation using SMOS and ESA-CCI that can be related to the important percentage of missing values. For the Issyl watershed, the satellite products show good correlations with the SMA model outputs (on average r=0.76) except for the SMOS product especially in winter. The highest mean correlations (i.e. averaged for all the different products) are found during fall in the Rheraya basin, with r=0.61 with in situ data and r=0.58 with SMA soil moisture. It should be noted that correlations with SMA outputs in summer are similar with r=0.59. For the Issyl basin, the correlations are also higher in the fall with a mean r=0.87 for the SMA model. The ERA5 product shows good correlations for most seasons. Complementary to this comparison of the different soil moisture products, an Extended Collocation Analysis has also been performed, comforting the results obtained (see supplementary materials).

**4.4 Calibration of the event-based hydrological model**

Calibration results (Table 6) on the individual flood events of Table 2 show that the difference between the values of the potential maximum soil moisture retention (S) of each basin is very important with larger values for the Issyl basin where the soil depth is prominent. We noticed that the temporal variability of soil moisture can be important between two successive events like the events of 02/04/2012 and 05/04/2012 for the Issyl basin. The SCS-CN model reproduces well the floods of the Rheraya basin with average Ns of 0.67 and bias on runoff peak (BIAS$_Q$) of 4% (Table 6). The SCS-CN model in calibration is able to reproduce the shape of the different flood events even for the most complex ones (21/04/2014 and 22/11/2014). Similarly, for the Issyl basin the SCS-CN model gives good results with average Ns of 0.66 and an average bias on runoff peak of 6.93%. The simulated hydrographs are in good agreement with the observations. The lower Ns coefficients obtained for the 23/01/2014 event in the Rheraya and for the 03/04/2011 and 28/09/2012 events in the Issyl basin are caused by a slight shift in the hydrograph probably due to a time lag in instantaneous precipitation measurements. For the Clark

433    Unit Hydrograph model, the averages of calibrated Tc and Sc parameters are considered for validation

434    (Sc = 1.42 and 2.54 hours and Tc = 2.85 and 3.64 hours for Rheraya and Issyl respectively).

435

436    The S parameters of the hydrological models, for the two basins, are then compared to the soil moisture

437    products. For the Rheraya basin, there are significant correlations of the S parameter with in-situ soil

438    moisture data, ERA5 and SMOS-IC (Table 7). The correlations using observed soil moisture, ESA-CCI

439    and SMOS data can be computed with only 8 and 6 events respectively, due to the presence of missing

440    values. The time step of the soil moisture data in the Rheraya basin seems to play a key role in the

441    representation of soil moisture conditions. Indeed, the daily time step shows a weakness to effectively

442    represent the antecedent soil moisture conditions in the SCS model, which indicates the rapid change of

443    soil moisture content in such a semi-arid mountainous basin. For the Issyl basin, ESA-CCI is the only

444    satellite product that is significantly correlated to the S parameter at the daily time step. The ERA5

445    product is also significantly correlated with the S parameter but at the hourly time step. The daily output

446    of the SMA model is also able to estimate the initial condition of the model for the Issyl basin, with a

447    correlation of -0.69 with S. Interestingly, the SMA model does not provide a good performance in the

448    Rheraya basin. It can be due to the fact that in such a mountainous basin, there is a strong spatial

449    variability of rainfall and it is difficult to obtain reliable precipitation estimates for continuous

450    simulations (Chapponiere et al., 2005).

451

452    **4.5 Validation of the event-based hydrological model**

453

454    The validation of the event-based hydrological model is performed on the events of Rheraya and Issyl

455    using only the soil moisture datasets that show relatively good correlations with the initial condition (S)

456    of the model from Table 8. These products include SMOS-IC, ERA5 and observed soil moisture for the

457    Rheraya, and ESA-CCI, ERA5, SMOS and SMA for Issyl. The validation of the event-based model is

458    performed with S calculated from the linear equation obtained from the correlation analysis between the

459    different soil moisture products and the calibrated parameter S. The validation results show that for the

460    Rheraya basin the events are well validated using both daily (Figure 6) and hourly (Figure 7) time step

461    of soil moisture products. The best validation result at the daily time step is obtained with SMOS-IC

462    with an average Ns of 0.58 for all events (median Ns =0.63). This result should be compared with the

463    results found in the previous sections where SMOS-IC showed the best correlations with observed soil

464    moisture. ASCAT and ERA5 show similar results in term of average Ns (~0.45). On the contrary, the

465    daily observed soil moisture shows a lower performance with an average Ns of 0.25 (median Ns =0.49).

466    The hourly time step enhanced the performance of the model, with an average Ns using the ERA5

467    product of 0.64 (median Ns = 0.73) and also a better performance with the hourly in-situ data with mean

468    Ns = 0.54 (median Ns = 0.61). These results show that the hourly time step better represents the

469    saturation content before the flood events in this basin. For the Issyl, the validation results are quite

470  different (Figure 8). For only 5 events (the 03/04/2011, 02/05/2011, 19/05/2011, 05/04/2012 and
471  25/03/2015) the event-based model can be validated using the ERA5 hourly data with an average Ns
472  coefficient of 0.46. For the events of the 16/05/2011 and 06/06/2011, an important spatial variability of
473  precipitation is observed, with no precipitation in the PQI station. In addition to these events, the flood
474  of the 28/09/2012 showed an overestimation of the validated value of S compared to the calibrated value.
475  This overestimation is related to the ERA5 estimation that considers the soil more saturated than it is.
476  For all other events and with different soil moisture products the Ns coefficients are negative and the
477  hydrographs not adequately reproduced. These validation results should be put in perspective with the
478  fact that the Issyl basin has a land use characterized by agricultural activities with possible large water
479  uptake in the diver channel during floods for irrigation. Some simple methods to compensate for the
480  water losses due to irrigation, such as the application of a varying percentage of runoff added to the
481  observed discharge to compensate the part of water lost for irrigation, have been tested but with no
482  improvement of the results. This is probably because the quantity taken for irrigation is not constant
483  from one event to another depending on the farmer needs, as shown by field surveys, and this amount
484  may also depend on discharge thresholds.

485

486  **5 Conclusions**

487

488  This study performed an evaluation of different soil moisture products (ASCAT, ESA-CCI, SMOS,
489  SMOS-IC and ERA5) using in-situ measurements and a Soil Moisture Accounting model (SMA) over
490  two basins located in the Moroccan High Atlas in order to estimate the initial soil moisture conditions
491  before flood events. The results indicated that the SMOS-IC product is well correlated with both the in-
492  situ soil moisture measurements and simulated soil moisture from the SMA model over the two basins.
493  Beside satellite products, the new ERA5 reanalysis reproduced also well the in-situ measurements over
494  the mountainous basin, which indicates the robustness of this product to estimate soil moisture in these
495  semi-arid environments. The seasonal analysis showed for both basins that the highest correlations are
496  found in autumn, which encourages the use of these remote sensing products for flood forecasting
497  because the majority of events occur in autumn and early winter in these regions (El Khalki et al., 2018).
498  One of the main finding of the present study is that different products, in particular SMOS-IC, ASCAT
499  and ERA5, are efficient to estimate the initial soil moisture conditions in an event-based hydrological
500  model, that could improve the forecasting capability in data-scare environments.

501

502  This study also showed that the hourly temporal resolution for soil moisture provides a better estimate
503  of antecedent wetness conditions before flood events. Indeed, the use of hourly soil moisture
504  measurements or ERA5 provided better performance than daily soil moisture to estimate the initial
505  condition of the hydrological model. These results indicate that the temporal variability of soil moisture
506  in these semi-arid basins under high evapotranspiration rates can be very important, causing a quick

decay of soil moisture after a rainfall event. For this type of basin, the use of soil moisture products with an hourly temporal resolution could be required to estimate with accuracy the soil moisture content prior to flood events. This constitute a research challenge to monitor soil moisture at the sub-daily timescale without ground measurements, since most remote sensing products at present are not available at the hourly time step. As shown by this study, atmospheric reanalysis coupled with a land surface model, such as ERA5, could provide a valuable alternative, in particular since the resolution of these products is constantly improving along with a more realistic representation of water balance.

For the catchment that is the most influenced by agricultural activities, the Issyl basin located nearby Marrakech, the water uptake for irrigation made difficult the validation of the hydrological model. The model overestimates runoff for some flood events, since the water uptake during floods from the river channel by small artisanal structures is not monitored and thus cannot be represented in the hydrological model. This example shows the difficulty in the implementation of a flood forecasting system in such basin without a good knowledge on the human influences on river discharge. This situation is not a particular case but deemed common in semi-arid areas where rivers with a high risk of flooding are also a substantial water resource for agriculture. Therefore, as shown by our results, a hydrological model that is not accounting for water use and irrigation may not be efficient at reproducing flood events in an operational context. The resolution of this issue would require the development of an irrigation monitoring system, that would need intensive field surveys and mapping but also the agreement of the local farmers that benefit from this system.

This study is a first step towards the development of operational flood forecasting systems in semi-arid North Africa basins highly impacted by floods. Indeed, the evaluation of the most suitable satellite or reanalysis products to estimate soil moisture for the monitoring of the basin saturation conditions before floods is a necessary first step prior to implement flood warning systems based on rainfall and soil moisture thresholds or coupled hydro-meteorological modeling (Javelle et al., 2016; Norbiato et al., 2008). Three important aspects that should be addressed in further research aiming at developing a flood forecasting system are: (1) the application of assimilation methods to correct the initial soil moisture condition of the basin and to increase the latency of soil moisture by using the observed discharge before the flood event (Coustau et al., 2013). (2) the joint assimilation of soil moisture and snow cover in order to better predict floods in the mountainous basins (Baba et al., 2018; Koster et al., 2010) and (3) the selection of soil moisture data based on the latency of soil moisture products. For instance, the ERA5 reanalysis is available within 5-days latency when ASCAT or SMOS satellite products could be available with 3-hours latency. With the issue of the latency to obtain some products, it should be noted also that the mismatch of spatial resolution between large scale remote sensing products and very local small-scale applications could be an additional issue. Prior to these developments, this type of evaluation should be generalized in Morocco and other sites in North Africa where soil moisture measurements are

available, for the development of reliable flood forecasting systems using the outputs of meteorological models.

**Author Contributions:** E.E. performed the analysis and wrote the paper, Y.T. designed the analysis and wrote the paper, C.M. and L.B. designed the analysis and contributed to the paper, C.M. performed the TC analysis, and M.S., V.S., S.G. contributed to the paper

**Acknowledgments:** This research has been conducted in TREMA International Joint Laboratory (https://www.lmi-trema.ma/) funded by the University Cadi Ayyad of Marrakech and the French IRD. This work is a contribution to the HYdrological cycle in The Mediterranean EXperiment (HyMeX) program, through INSU-MISTRALS support. The financial support provided by the ERASMUS+ mobility and the Centre National de la Recherche Scientifique et Technique (CNRST) are gratefully acknowledged. Thanks are due to the hydrological basin agency Tensift (ABHT) and to the LMI TREMA for providing the data. The Authors would like to thank Professor Khalid Chaouch for his English revision and the associated Editor Eric Martin and two anonymous reviewers that helped to improve the manuscript.

**Conflicts of Interest:** The authors declare no conflict of interest.

**References**

Al-Yaari, A., Wigneron, J.-P., Ducharne, A., Kerr, Y. H., Wagner, W., De Lannoy, G., Reichle, R., Al Bitar, A., Dorigo, W., Richaume, P. and Mialon, A.: Global-scale comparison of passive (SMOS) and active (ASCAT) satellite based microwave soil moisture retrievals with soil moisture simulations (MERRA-Land), Remote Sens. Environ., 152, 614–626, doi:10.1016/J.RSE.2014.07.013, 2014.

El Alaoui El Fels, A., Bachnou, A. and Alaa, N.: Combination of GIS and mathematical modeling to predict floods in semiarid areas: case of Rheraya watershed (Western High Atlas, Morocco), Arab. J. Geosci., 10(24), 554, doi:10.1007/s12517-017-3345-x, 2017.

Albergel, C., Calvet, J.-C., De Rosnay, P., Balsamo, G., Wagner, W., Hasenauer, S., Naeimi, V., Martin, E., Bazile, E., Bouyssel, F. and Mahfouf, J.-F.: Hydrology and Earth System Sciences Cross-evaluation of modelled and remotely sensed surface soil moisture with in situ data in southwestern France, Hydrol. Earth Syst. Sci, 14, 2177–2191, doi:10.5194/hess-14-2177-2010, 2010.

Albergel, C., Dorigo, W., Balsamo, G., Muñoz-Sabater, J., de Rosnay, P., Isaksen, L., Brocca, L., de Jeu, R. and Wagner, W.: Monitoring multi-decadal satellite earth observation of soil moisture products through land surface reanalyses, Remote Sens. Environ., 138, 77–89, doi:10.1016/J.RSE.2013.07.009, 2013.

Albergel, C., Dutra, E., Munier, S., Calvet, J.-C., Munoz-Sabater, J., de Rosnay, P. and Balsamo, G.: ERA-5 and ERA-Interim driven ISBA land surface model simulations: which one performs better?,

Hydrol. Earth Syst. Sci., 22(6), 3515–3532, doi:10.5194/hess-22-3515-2018, 2018.

Anctil, F., Michel, C., Perrin, C. and Andréassian, V.: A soil moisture index as an auxiliary ANN input for stream flow forecasting, J. Hydrol., 286(1–4), 155–167, doi:10.1016/J.JHYDROL.2003.09.006, 2004.

Baba, M. W., Gascoin, S. and Hanich, L.: Assimilation of Sentinel-2 data into a snowpack model in the High Atlas of Morocco, Remote Sens., 10(12), 1–23, doi:10.3390/rs10121982, 2018.

Bennani, O., Druon, E., Leone, F., Tramblay, Y. and Saidi, M. E. M.: A spatial and integrated flood risk diagnosis, Disaster Prev. Manag. An Int. J., DPM-12-2018-0379, doi:10.1108/DPM-12-2018-0379, 2019.

Boudhar, A., Hanich, L., Boulet, G., Duchemin, B., Berjamy, B. and Chehbouni, A.: Evaluation of the Snowmelt Runoff Model in the Moroccan High Atlas Mountains using two snow-cover estimates, Hydrol. Sci. J., 54(6), 1094–1113, doi:10.1623/hysj.54.6.1094, 2009.

Bouimouass, H., Fakir, Y., Tweed, S., and Leblanc, M.: Groundwater recharge sources in semiarid irrigated mountain fronts, Hydrological Processes, 34(7), 1598–1615. https://doi.org/10.1002/hyp.13685, 2020

Boumenni, H., Bachnou, A. and Alaa, N. E.: The rainfall-runoff model GR4J optimization of parameter by genetic algorithms and Gauss-Newton method: application for the watershed Ourika (High Atlas, Morocco), Arab. J. Geosci., 10(15), 343, doi:10.1007/s12517-017-3086-x, 2017.

Brocca, L., Melone, F., Moramarco, T. and Morbidelli, R.: Antecedent wetness conditions based on ERS scatterometer data, J. Hydrol., doi:10.1016/j.jhydrol.2008.10.007, 2009a.

Brocca, L., Melone, F., Moramarco, T. and Morbidelli, R.: Soil moisture temporal stability over experimental areas in Central Italy, Geoderma, doi:10.1016/j.geoderma.2008.11.004, 2009b.

Brocca, L., Melone, F., Moramarco, T. and Morbidelli, R.: Spatial-temporal variability of soil moisture and its estimation across scales, Water Resour. Res., doi:10.1029/2009WR008016, 2010.

Brocca, L., Hasenauer, S., Lacava, T., Melone, F., Moramarco, T., Wagner, W., Dorigo, W., Matgen, P., Martínez-Fernández, J., Llorens, P., Latron, J., Martin, C. and Bittelli, M.: Soil moisture estimation through ASCAT and AMSR-E sensors: An intercomparison and validation study across Europe, Remote Sens. Environ., doi:10.1016/j.rse.2011.08.003, 2011.

Brocca, L., Crow, W. T., Ciabatta, L., Massari, C., De Rosnay, P., Enenkel, M., Hahn, S., Amarnath, G., Camici, S., Tarpanelli, A. and Wagner, W.: A Review of the Applications of ASCAT Soil Moisture Products, IEEE J. Sel. Top. Appl. Earth Obs. Remote Sens., 10(5), 2285–2306, doi:10.1109/JSTARS.2017.2651140, 2017.

Chaponnière, A., Boulet, G., Chehbouni, A. and Aresmouk, M.: Understanding hydrological processes with scarce data in a mountain environment, Hydrol. Process., 22(12), 1908–1921, doi:10.1002/hyp.6775, 2008.

Coustau, M., Ricci, S., Borrell-Estupina, V., Bouvier, C. and Thual, O.: Benefits and limitations of data assimilation for discharge forecasting using an event-based rainfall–runoff model, Nat. Hazards Earth

Syst. Sci., 13(3), 583–596, doi:10.5194/nhess-13-583-2013, 2013.

Creutin, J.-D. and Borga, M.: Radar hydrology modifies the monitoring of flash-flood hazard, Hydrol. Process., 17(7), 1453–1456, doi:10.1002/hyp.5122, 2003.

Dakhlaoui, H., Seibert, J. and Hakala, K.: Sensitivity of discharge projections to potential evapotranspiration estimation in Northern Tunisia, Reg. Environ. Chang., 20(2), 1–12, doi:10.1007/s10113-020-01615-8, 2020.

Van doninck, J., Peters, J., Lievens, H., De Baets, B. and Verhoest, N. E. C.: Accounting for seasonality in a soil moisture change detection algorithm for ASAR Wide Swath time series, Hydrol. Earth Syst. Sci., 16(3), 773–786, doi:10.5194/hess-16-773-2012, 2012.

Dorigo, W., de Jeu, R., Chung, D., Parinussa, R., Liu, Y., Wagner, W. and Fernández-Prieto, D.: Evaluating global trends (1988-2010) in harmonized multi-satellite surface soil moisture, Geophys. Res. Lett., 39(18), doi:10.1029/2012GL052988, 2012.

Dorigo, W., Wagner, W., Albergel, C., Albrecht, F., Balsamo, G., Brocca, L., Chung, D., Ertl, M., Forkel, M., Gruber, A., Haas, E., Hamer, P. D., Hirschi, M., Ikonen, J., de Jeu, R., Kidd, R., Lahoz, W., Liu, Y. Y., Miralles, D., Mistelbauer, T., Nicolai-Shaw, N., Parinussa, R., Pratola, C., Reimer, C., van der Schalie, R., Seneviratne, S. I., Smolander, T. and Lecomte, P.: ESA CCI Soil Moisture for improved Earth system understanding: State-of-the art and future directions, Remote Sens. Environ., 203, 185–215, doi:10.1016/j.rse.2017.07.001, 2017.

Dorigo, W. A., Gruber, A., De Jeu, R. A. M., Wagner, W., Stacke, T., Loew, A., Albergel, C., Brocca, L., Chung, D., Parinussa, R. M. and Kidd, R.: Evaluation of the ESA CCI soil moisture product using ground-based observations, , doi:10.1016/j.rse.2014.07.023, 2015.

Fernandez-Moran, R., Wigneron, J.-P., De Lannoy, G., Lopez-Baeza, E., Parrens, M., Mialon, A., Mahmoodi, A., Al-Yaari, A., Bircher, S., Al Bitar, A., Richaume, P. and Kerr, Y.: A new calibration of the effective scattering albedo and soil roughness parameters in the SMOS SM retrieval algorithm, Int. J. Appl. Earth Obs. Geoinf., 62, 27–38, doi:10.1016/J.JAG.2017.05.013, 2017.

Gaume, E., Livet, M., Desbordes, M. and Villeneuve, J.-P.: Hydrological analysis of the river Aude, France, flash flood on 12 and 13 November 1999, J. Hydrol., 286(1–4), 135–154, doi:10.1016/J.JHYDROL.2003.09.015, 2004.

Gruber, A., Dorigo, W. A., Crow, W. and Wagner, W.: Triple Collocation-Based Merging of Satellite Soil Moisture Retrievals, IEEE Trans. Geosci. Remote Sens., 55(12), 6780–6792, doi:10.1109/TGRS.2017.2734070, 2017.

Gruber, A., Scanlon, T., Van Der Schalie, R., Wagner, W. and Dorigo, W.: Evolution of the ESA CCI Soil Moisture climate data records and their underlying merging methodology, Earth Syst. Sci. Data, 11, 717–739, doi:10.5194/essd-11-717-2019, 2019.

Hajhouji, Y., Simonneaux, V., Gascoin, S., Fakir, Y., Richard, B., Chehbouni, A. and Boudhar, A.: Modélisation pluie-débit et analyse du régime d'un bassin versant semi-aride sous influence nivale. Cas du bassin versant du Rheraya (Haut Atlas, Maroc), La Houille Blanche, (3), 49–62,

doi:10.1051/lhb/2018032, 2018.

Hwang, S. O., Park, J. and Kim, H. M.: Effect of hydrometeor species on very-short-range simulations of precipitation using ERA5, Atmos. Res., 218(December 2018), 245–256, doi:10.1016/j.atmosres.2018.12.008, 2019.

Jackson, T. J., Cosh, M. H., Bindlish, R., Starks, P. J., Bosch, D. D., Seyfried, M., Goodrich, D. C., Moran, M. S. and Du, J.: Validation of advanced microwave scanning radiometer soil moisture products, IEEE Trans. Geosci. Remote Sens., 48(12), 4256–4272, doi:10.1109/TGRS.2010.2051035, 2010.

Jarlan, L., Khabba, S., Er-Raki, S., Le Page, M., Hanich, L., Fakir, Y., Merlin, O., Mangiarotti, S., Gascoin, S., Ezzahar, J., Kharrou, M. H., Berjamy, B., Saaïdi, A., Boudhar, A., Benkaddour, A., Laftouhi, N., Abaoui, J., Tavernier, A., Boulet, G., Simonneaux, V., Driouech, F., El Adnani, M., El Fazziki, A., Amenzou, N., Raibi, F., El Mandour, A., Ibouh, H., Le Dantec, V., Habets, F., Tramblay, Y., Mougenot, B., Leblanc, M., El Faïz, M., Drapeau, L., Coudert, B., Hagolle, O., Filali, N., Belaqziz, S., Marchane, A., Szczypta, C., Toumi, J., Diarra, A., Aouade, G., Hajhouji, Y., Nassah, H., Bigeard, G., Chirouze, J., Boukhari, K., Abourida, A., Richard, B., Fanise, P., Kasbani, M., Chakir, A., Zribi, M., Marah, H., Naimi, A., Mokssit, A., Kerr, Y. and Escadafal, R.: Remote Sensing of Water Resources in Semi-Arid Mediterranean Areas: the joint international laboratory TREMA, Int. J. Remote Sens., 36(19–20), 4879–4917, doi:10.1080/01431161.2015.1093198, 2015.

Javelle, P., Fouchier, C., Arnaud, P. and Lavabre, J.: Flash flood warning at ungauged locations using radar rainfall and antecedent soil moisture estimations, J. Hydrol., doi:10.1016/j.jhydrol.2010.03.032, 2010.

Javelle, P., Organde, D., Demargne, J., Saint-Martin, C., Saint-Aubin, C. de, Garandeau, L. and Janet, B.: Setting up a French national flash flood warning system for ungauged catchments based on the AIGA method, E3S Web Conf., 7, 18010, doi:10.1051/E3SCONF/20160718010, 2016.

Jiang, D. and Wang, K.: The role of satellite-based remote sensing in improving simulated streamflow: A review, Water (Switzerland), 11(8), doi:10.3390/w11081615, 2019.

Kerr, Y. H., Waldteufel, P., Wigneron, J.-P., Martinuzzi, J.-M., Font, J. and Berger, M.: Soil Moisture Retrieval from Space: The Soil Moisture and Ocean Salinity (SMOS) Mission. [online] Available from: https://pdfs.semanticscholar.org/089c/4c73617a96fd33ef7be538d2c3899b2075c2.pdf (Accessed 20 August 2019), 2001.

Kerr, Y. H., Waldteufel, P., Richaume, P., Wigneron, J. P., Ferrazzoli, P., Mahmoodi, A., Al Bitar, A., Cabot, F., Gruhier, C., Juglea, S. E., Leroux, D., Mialon, A. and Delwart, S.: The SMOS Soil Moisture Retrieval Algorithm, IEEE Trans. Geosci. Remote Sens., 50(5), 1384–1403, doi:10.1109/TGRS.2012.2184548, 2012.

Khabba, S., Jarlan, L., Er-Raki, S., Le Page, M., Ezzahar, J., Boulet, G., Simonneaux, V., Kharrou, M. H., Hanich, L. and Chehbouni, G.: The SudMed Program and the Joint International Laboratory TREMA: A Decade of Water Transfer Study in the Soil-plant-atmosphere System over Irrigated Crops in Semi-arid Area, Procedia Environ. Sci., 19, 524–533, doi:10.1016/J.PROENV.2013.06.059, 2013.

692     El Khalki, E. M., Tramblay, Y., El Mehdi Saidi, M., Bouvier, C., Hanich, L., Benrhanem, M. and

693     Alaouri, M.: Comparison of modeling approaches for flood forecasting in the High Atlas Mountains of

694     Morocco, Arab. J. Geosci., 11(15), doi:10.1007/s12517-018-3752-7, 2018.

695     Koster, R. D., Guo, Z., Yang, R., Dirmeyer, P. A., Mitchell, K., Puma, M. J., Koster, R. D., Guo, Z.,

696     Yang, R., Dirmeyer, P. A., Mitchell, K. and Puma, M. J.: On the Nature of Soil Moisture in Land Surface

697     Models, J. Clim., 22(16), 4322–4335, doi:10.1175/2009JCLI2832.1, 2009.

698     Koster, R. D., Mahanama, S. P. P., Livneh, B., Lettenmaier, D. P. and Reichle, R. H.: Skill in streamflow

699     forecasts derived from large-scale estimates of soil moisture and snow, Nat. Geosci., 3(9), 613–616,

700     doi:10.1038/ngeo944, 2010.

701     Liu, Y. Y., Parinussa, R. M., Dorigo, W. A., De Jeu, R. A. M., Wagner, W., M. Van Dijk, A. I. J.,

702     McCabe, M. F. and Evans, J. P.: Developing an improved soil moisture dataset by blending passive and

703     active microwave satellite-based retrievals, Hydrol. Earth Syst. Sci., doi:10.5194/hess-15-425-2011,

704     2011a.

705     Liu, Y. Y., Parinussa, R. M., Dorigo, W. A., De Jeu, R. A. M., Wagner, W., van Dijk, A. I. J. M.,

706     McCabe, M. F. and Evans, J. P.: Developing an improved soil moisture dataset by blending passive and

707     active microwave satellite-based retrievals, Hydrol. Earth Syst. Sci., 15(2), 425–436, doi:10.5194/hess-

708     15-425-2011, 2011b.

709     Loew, A. and Mauser, W.: On the disaggregation of passive microwave soil moisture data using A Priori

710     knowledge of temporally persistent soil moisture fields, IEEE Trans. Geosci. Remote Sens., 46(3), 819–

711     834, doi:10.1109/TGRS.2007.914800, 2008.

712     Loew, A. and Schlenz, F.: A dynamic approach for evaluating coarse scale satellite soil moisture

713     products, Hydrol. Earth Syst. Sci., 15(1), 75–90, doi:10.5194/hess-15-75-2011, 2011.

714     Ma, H., Zeng, J., Chen, N., Zhang, X., Cosh, M. H. and Wang, W.: Satellite surface soil moisture from

715     SMAP, SMOS, AMSR2 and ESA CCI: A comprehensive assessment using global ground-based

716     observations, Remote Sens. Environ., 231, doi:10.1016/j.rse.2019.111215, 2019.

717     Mahto, S. S. and Mishra, V.: Does ERA-5 Outperform Other Reanalysis Products for Hydrologic

718     Applications in India?, J. Geophys. Res. Atmos., 124(16), 9423–9441, doi:10.1029/2019JD031155,

719     2019.

720     Marchandise, A. and Viel, C.: Utilisation des indices d'humidité de la chaîne Safran-Isba-Modcou de

721     Météo-France pour la vigilance et la prévision opérationnelle des crues, La Houille Blanche,

722     doi:10.1051/lhb/2009075, 2010.

723     Marchane, A., Tramblay, Y., Hanich, L., Ruelland, D. and Jarlan, L.: Climate change impacts on surface

724     water resources in the Rheraya catchment (High Atlas, Morocco), Hydrol. Sci. J., 62(6), 979–995,

725     doi:10.1080/02626667.2017.1283042, 2017.

726     Martínez-Fernández, J. and Ceballos, A.: Mean soil moisture estimation using temporal stability

727     analysis, J. Hydrol., 312(1–4), 28–38, doi:10.1016/j.jhydrol.2005.02.007, 2005.

728     Massari, C., Brocca, L., Moramarco, T., Tramblay, Y. and Didon Lescot, J.-F.: Potential of soil moisture

729 observations in flood modelling: estimating initial conditions and correcting rainfall, Adv. Water

730 Resour., 74, 44–53, doi:10.1016/j.advwatres.2014.08.004, 2014.

731 Massari, C., Brocca, L., Ciabatta, L., Moramarco, T., Gabellani, S., Albergel, C., De Rosnay, P., Puca,

732 S. and Wagner, W.: The Use of H-SAF Soil Moisture Products for Operational Hydrology: Flood

733 Modelling over Italy, Hydrology, 2(1), 2–22, doi:10.3390/hydrology2010002, 2015.

734 Merheb, M., Moussa, R., Abdallah, C., Colin, F., Perrin, C. and Baghdadi, N.: Hydrological response

735 characteristics of Mediterranean catchments at different time scales: a meta-analysis, ,

736 doi:10.1080/02626667.2016.1140174, 2016.

737 Miliani, F., Ravazzani, G. and Mancini, M.: Adaptation of Precipitation Index for the Estimation of

738 Antecedent Moisture Condition in Large Mountainous Basins, J. Hydrol. Eng., 16(3), 218–227,

739 doi:10.1061/(ASCE)HE.1943-5584.0000307, 2011.

740 Miralles, D. G., Crow, W. T. and Cosh, M. H.: Estimating Spatial Sampling Errors in Coarse-Scale Soil

741 Moisture Estimates Derived from Point-Scale Observations, J. Hydrometeorol., 11(6), 1423–1429,

742 doi:10.1175/2010JHM1285.1, 2010.

743 Nash, J. E. and Sutcliffe, J. V.: River flow forecasting through conceptual models part I — A discussion

744 of principles, J. Hydrol., 10(3), 282–290, doi:10.1016/0022-1694(70)90255-6, 1970.

745 Norbiato, D., Borga, M., Degli Esposti, S., Anquetin, S. and Gaume, E.: Flash flood warning based on

746 rainfall thresholds and soil moisture conditions: An assessment for gauged and ungauged basins, J.

747 Hydrol., doi:10.1016/j.jhydrol.2008.08.023, 2008.

748 Ochsner, T. E., Cosh, M. H., Cuenca, R. H., Dorigo, W. A., Draper, C. S., Hagimoto, Y., Kerr, Y. H.,

749 Njoku, E. G., Small, E. E., Zreda, M. and Larson, K. M.: State of the Art in Large-Scale Soil Moisture

750 Monitoring, Soil Sci. Soc. Am. J., 77(6), 1888, doi:10.2136/sssaj2013.03.0093, 2013.

751 Olauson, J.: ERA5: The new champion of wind power modelling?, Renew. Energy, 126, 322–331,

752 doi:10.1016/j.renene.2018.03.056, 2018.

753 Oudin, L., Michel, C. and Anctil, F.: Which potential evapotranspiration input for a lumped rainfall-

754 runoff model?: Part 1—Can rainfall-runoff models effectively handle detailed potential

755 evapotranspiration inputs?, J. Hydrol., 303(1–4), 275–289, doi:10.1016/J.JHYDROL.2004.08.025,

756 2005.

757 Pérennès, J. J.: L'eau et les hommes au Maghreb. Contribution à une politique de l'eau en Méditerranée,

758 Rev. Tiers Monde, 35(137), 231–232 [online] Available from: https://www.persee.fr/doc/tiers_0040-

759 7356_1994_num_35_137_4870_t1_0231_0000_5 (Accessed 7 October 2019), 1994.

760 Saidi, M. E. M., Daoudi, L., Aresmouk, M. E. H. and Blali, A.: Rôle du milieu physique dans

761 l'amplification des crues en milieu montagnard: exemple de la crue du 17 août 1995 dans la vallée de

762 l'Ourika (Haut-Atlas, Maroc), Sécheresse, v. 14(2) p(April 2003) [online] Available from:

763 http://agris.fao.org/agris-search/search/display.do?f=2003/FR/FR03035.xml;FR2003003547, 2003.

764 Schulte, R. P. O., Diamond, J., Finkele, K., Holden, N. M. and Brereton, A. J.: Predicting the Soil

765 Moisture Conditions of Irish Grasslands, Irish J. Agric. Food Res., 44, 95–110, doi:10.2307/25562535,

766    2005.

767    Tramblay, Y., Bouvier, C., Crespy, A. and Marchandise, A.: Improvement of flash flood modelling

768    using spatial patterns of rainfall : a case study in southern France, , 2(October), 172–178, 2010.

769    Tramblay, Y., Bouvier, C., Ayral, P. A. and Marchandise, A.: Impact of rainfall spatial distribution on

770    rainfall-runoff modelling efficiency and initial soil moisture conditions estimation, Nat. Hazards Earth

771    Syst. Sci., doi:10.5194/nhess-11-157-2011, 2011.

772    Tramblay, Y., Bouaicha, R., Brocca, L., Dorigo, W., Bouvier, C., Camici, S. and Servat, E.: Estimation

773    of antecedent wetness conditions for flood modelling in northern Morocco, Hydrol. Earth Syst. Sci.,

774    16(11), 4375–4386, doi:10.5194/hess-16-4375-2012, 2012.

775    Tramblay, Y., Ruelland, D., Somot, S., Bouaicha, R. and Servat, E.: High-resolution Med-CORDEX

776    regional climate model simulations for hydrological impact studies: A first evaluation of the ALADIN-

777    Climate model in Morocco, Hydrol. Earth Syst. Sci., 17(10), 3721–3739, doi:10.5194/hess-17-3721-

778    2013, 2013.

779    Tuttle, S. E. and Salvucci, G. D.: A new approach for validating satellite estimates of soil moisture using

780    large-scale precipitation: Comparing AMSR-E products, Remote Sens. Environ., 142, 207–222,

781    doi:10.1016/j.rse.2013.12.002, 2014.

782    US Army Corps of Engineers: Hydrologic Modelling System HEC-HMS., 2015.

783    Vinet, F., El Mehdi Saidi, M., Douvinet, J., Fehri, N., Nasrallah, W., Menad, W. and Mellas, S.: Sub-

784    chapter 3.4.1. Urbanization and land use as a driver of flood risk, in The Mediterranean region under

785    climate change, pp. 563–575, IRD Éditions., 2016.

786    Wagner, W., Pathe, C., Doubkova, M., Sabel, D., Bartsch, A., Hasenauer, S., Blöschl, G., Scipal, K.,

787    Martínez-Fernández, J. and Löw, A.: Temporal Stability of Soil Moisture and Radar Backscatter

788    Observed by the Advanced Synthetic Aperture Radar (ASAR), Sensors, 8(2), 1174–1197,

789    doi:10.3390/s80201174, 2008.

790    Wagner, W., Hahn, S., Kidd, R., Melzer, T., Bartalis, Z., Hasenauer, S., Figa-Saldaña, J., de Rosnay, P.,

791    Jann, A., Schneider, S., Komma, J., Kubu, G., Brugger, K., Aubrecht, C., Züger, J., Gangkofner, U.,

792    Kienberger, S., Brocca, L., Wang, Y., Blöschl, G., Eitzinger, J. and Steinnocher, K.: The ASCAT Soil

793    Moisture Product: A Review of its Specifications, Validation Results, and Emerging Applications,

794    Meteorol. Zeitschrift, 22(1), 5–33, doi:10.1127/0941-2948/2013/0399, 2013.

795    Western, A. W. and Blöschl, G.: On the spatial scaling of soil moisture., 1999.

796    Wigneron, J.-P., Kerr, Y., Waldteufel, P., Saleh, K., Escorihuela, M.-J., Richaume, P., Ferrazzoli, P., de

797    Rosnay, P., Gurney, R., Calvet, J.-C., Grant, J. P., Guglielmetti, M., Hornbuckle, B., Mätzler, C.,

798    Pellarin, T. and Schwank, M.: L-band Microwave Emission of the Biosphere (L-MEB) Model:

799    Description and calibration against experimental data sets over crop fields, Remote Sens. Environ.,

800    107(4), 639–655, doi:10.1016/J.RSE.2006.10.014, 2007.

801    Zema, Demetrio 1. Zema, D.A.; Labate, A.; Martino, D.; Zimbone, S.M. Comparing Different

802    Infiltration Methods of the HEC-HMS Model: The Case Study of the Mésima Torrent (Southern Italy).

803  L. Degrad. Dev. 2017, 28, 294–308.Antonio, Labate, A., Martino, D. and Zimbone, S. M.: Comparing

804  Different Infiltration Methods of the HEC-HMS Model: The Case Study of the Mésima Torrent

805  (Southern Italy), L. Degrad. Dev., 28(1), 294–308, doi:10.1002/ldr.2591, 2017.

806  Zeng, J., Li, Z., Chen, Q., Bi, H., Qiu, J. and Zou, P.: Evaluation of remotely sensed and reanalysis soil

807  moisture products over the Tibetan Plateau using in-situ observations, Remote Sens. Environ., 163, 91–

808  110, doi:10.1016/j.rse.2015.03.008, 2015.

809

810

811

812

813

814

815

816

817

818

819

820

821

822

823

824

825

826

827

828

829

830

831

832

833

834

835

836

837

838      **TABLES**

839

 **Table 1: Stations with observed precipitation and river discharge**

| Catchment | Gauges | Code | Altitude [m] | Source | Type | Time step | Period |
|---|---|---|---|---|---|---|---|
| Rheraya | Asni | PR1 | 1170 | LMI TREMA | | | |
| | Imskerbour | PR2 | 1416 | LMI TREMA | | | |
| | Matate | PR3 | 1753 | ABHT | | | |
| | Oukaimeden | PR4 | 3239 | LMI TREMA | P | 30min | 2008-2016 |
| | Tachedert | PR5 | 2336 | LMI TREMA | | | |
| | Tamatarte | PR6 | 1906 | ABHT | | | |
| | Armed | SMPR7 | 2030 | ABHT | | | |
| | Neltner | PR8 | 3177 | LMI TREMA | | | |
| | Tahnaout | QR | 990 | ABHT | Discharge | 10min | 2014 |
| Issyl | Ait Bouzguia | PQI1 | 623 | | Precipitation and discharge | 10 minutes | 2010-2015 |
| | Ouaguejdit | PI2 | 1039 | | Precipitation | | |

841

842

843

844

845

846

847

848

849

850

851

852

853

854

855

856

857

858

859

860

861

862

863 **Table 2: Characteristics of the selected flood events.**

**Rheraya**

|  | Max Discharge [m³/s] | Volume [10³ m³] | Precipitation Volume [10³ m³] | Runoff Coefficient [%] |
|---|---|---|---|---|
| 23/01/2014 | 17.1 | 459.2 | 2749.5 | 16.7 |
| 29/01/2014 | 39.7 | 602.8 | 2632.5 | 22.9 |
| 10/02/2014 | 19.2 | 543.2 | 2904.7 | 18.7 |
| 11/03/2014 | 19 | 557 | 1633.5 | 34.1 |
| 21/04/2014 | 38.2 | 1070 | 5431.5 | 19.7 |
| 21/09/2014 | 24.4 | 440.6 | 3363.8 | 13.1 |
| 05/11/2014 | 46.5 | 1027 | 5737.5 | 17.9 |
| 09/11/2014 | 42.2 | 869.3 | 4575.2 | 19 |
| 22/11/2014 | 99.5 | 3868.9 | 17586 | 22 |
| 28/11/2014 | 76.4 | 3797.2 | 11940.8 | 31.8 |
| **Issyl** | | | | |
| 25/03/2011 | 63.8 | 385.28 | 27520 | 1.4 |
| 03/04/2011 | 16.6 | 550.656 | 30592 | 1.8 |
| 29/04/2011 | 19.7 | 246.4 | 11200 | 2.2 |
| 02/05/2011 | 17.1 | 303.36 | 10112 | 3.0 |
| 16/05/2011 | 45.8 | 361.12 | 9760 | 3.7 |
| 19/05/2011 | 27.6 | 315.392 | 7168 | 4.4 |
| 06/06/2011 | 18.3 | 212.352 | 5056 | 4.2 |
| 02/04/2012 | 16.8 | 216.576 | 18048 | 1.2 |
| 05/04/2012 | 20 | 543.744 | 7552 | 7.2 |
| 28/09/2012 | 22.7 | 126.72 | 7040 | 1.8 |
| 05/04/2013 | 15.4 | 365.376 | 16608 | 2.2 |
| 28/11/2014 | 37.2 | 489.6 | 28800 | 1.7 |
| 25/03/2015 | 16.2 | 767.424 | 18272 | 4.2 |

864

865 **Table 3: Summary of the soil moisture products considered**

| Product | Type | Temporal resolution | Spatial resolution | Source |
|---|---|---|---|---|
| **ASCAT** | Active | 1 to 2 observations per day | 12.5 km (H115) | EUMETSAT project (http://hsaf.meteoam.it/) |
| **SMOS** | Passive | 1 observation per 2/3 days | 25 km (EASEv2) | CATDS, (https://www.catds.fr/) |
| **SMOS-IC** | Passive | Daily | 25 km (EASEv2) | Wigneron et al., 2007 |
| **ESA-CCI** | Combined | Daily | 25km | http://www.esa-soilmoisture-cci.org/ |
| **ERA5** | Reanalysis | Hourly | 31 km | Copernicus Climate Change Service (C3S), 2017 |

866

867 **Table 4: Percentage of missing values for the different soil moisture products between 2013 and 2016**

**Percentage of missing values**

|          | In-Situ | ASCAT | SMOS   | SMOS-IC | ESA-CCI | ERA5 |
|----------|---------|-------|--------|---------|---------|------|
| **Rheraya** | 12%   | 0%    | 18.70% | 6.82%   | 46%     | 0%   |
| **Issyl**   | -     | 0%    | 17.19% | 9.10%   | 2.20%   | 0%   |

**Table 5: Seasonal correlation between the different soil moisture data, in situ measurements and the SMA model (significant correlations are represented in bold)**

|         |            | Winter | Spring | Summer | Fall |
|---------|------------|--------|--------|--------|------|
|         |            | **Rheraya** | | | |
| In-situ | SMA A=8mm  | **0.82** | **0.83** | **0.67** | **0.75** |
| ASCAT   | In-situ    | **0.47** | -0.03 | 0.18 | **0.70** |
|         | SMA A=8mm  | **0.32** | 0.09 | **0.54** | **0.65** |
| SMOS    | In-situ    | 0.01 | **0.68** | **0.61** | 0.16 |
|         | SMA A=8mm  | -0.09 | **0.75** | **0.58** | **0.54** |
| SMOS-IC | In-situ    | **0.80** | **0.68** | **0.45** | **0.85** |
|         | SMA A=8mm  | **0.80** | **0.72** | **0.62** | **0.57** |
| ESACCI  | In-situ    | 0.12 | 0.28 | **0.41** | **0.60** |
|         | SMA A=8mm  | 0.15 | **0.30** | **0.67** | **0.51** |
| ERA5    | In-situ    | **0.74** | **0.73** | 0.04 | **0.73** |
|         | SMA A=8mm  | **0.86** | **0.76** | **0.54** | **0.65** |
| Mean    | In-situ    | 0.43 | 0.47 | 0.34 | 0.61 |
|         | SMA A=8mm  | 0.41 | 0.52 | 0.59 | 0.58 |
|         |            | **Issyl** | | | |
| ASCAT   |            | **0.77** | **0.86** | **0.70** | **0.90** |
| SMOS    |            | **0.39** | **0.76** | **0.47** | **0.74** |
| SMOS-IC | SMA A=30mm | **0.85** | **0.81** | **0.56** | **0.93** |
| ESACCI  |            | **0.70** | **0.89** | **0.77** | **0.89** |
| ERA5    |            | **0.88** | **0.82** | **0.70** | **0.88** |
| Mean    | SMA A=30mm | 0.72 | 0.83 | 0.64 | 0.87 |

**Table 6: Calibration results of SCS-CN model, S is the potential maximum soil moisture retention,**

**BIAS_Q is the difference between the observed and calibrated peak discharge of the event, BIAS_V is**

**the difference between the observed and calibrated volume of the event.**

| | Rheraya | | | | Issyl | | | | |
|---|---|---|---|---|---|---|---|---|---|
| **Events** | **S[mm]** | **Ns** | **BIAS_Q [%]** | **BIAS_V [%]** | **Events** | **S[mm]** | **Ns** | **BIAS_Q [%]** | **BIAS_V [%]** |
| 23/01/2014 | 19.1 | -0.58 | 1.18 | -5.76 | 25/03/2011 | 679.8 | 0,83 | 29,94 | -13,5 |
| 29/01/2014 | 24.5 | 0.87 | 6.43 | 29.14 | 03/04/2011 | 730.5 | 0,02 | -12,05 | 27,93 |
| 10/02/2014 | 34.6 | 0.71 | -4.00 | 2.85 | 29/04/2011 | 218.1 | 0,83 | 0 | 10,36 |
| 11/03/2014 | 9.5 | 0.61 | -17.39 | 2.57 | 02/05/2011 | 113 | 0,91 | -0,58 | 44,39 |
| 21/04/2014 | 55.8 | 0.73 | 6.41 | 2.30 | 16/05/2011 | 176.5 | 0,61 | 17,69 | -26,31 |
| 21/09/2014 | 34.6 | 0.77 | 27.08 | -6.87 | 19/05/2011 | 136.7 | 0,87 | 1,09 | 9,64 |
| 05/11/2014 | 39.6 | 0.97 | 15.38 | 0.88 | 06/06/2011 | 108.8 | 0,75 | 0 | -5,38 |
| 09/11/2014 | 40.7 | 0.83 | 6.30 | -0.32 | 02/04/2012 | 440.3 | 0,56 | 0 | 15,26 |
| 22/11/2014 | 43.1 | 0.78 | -5.06 | 2.38 | 05/04/2012 | 125.1 | 0,56 | 13,5 | -1,91 |
| 28/11/2014 | 71.6 | 0.97 | 3.66 | -6.22 | 28/09/2012 | 159.7 | 0,11 | 32,16 | 23,41 |
| | | | | | 05/04/2013 | 388.2 | 0,90 | 6,49 | -4,16 |
| | | | | | 28/11/2014 | 254 | 0,74 | 1,88 | 0,71 |
| | | | | | 25/03/2015 | 356.6 | 0,89 | 0 | 12,32 |
| Mean | | 0.67 | 4.00 | 2.09 | Mean | | 0,66 | 6,93 | 7,14 |
| Median | | 0.77 | 4.98 | 1.59 | Median | | 0,75 | 1,09 | 9,64 |

883

884

**Table 7: Correlation between the different soil moisture products and the S parameter of the SCS-CN hydrological model**

| | Rheraya | | Issyl | |
|---|---|---|---|---|
| | **S** | **Number of events** | **S** | **Number of events** |
| In-situ [Daily] | -0.71 | 8 | - | - |
| In-situ [Hourly] | -0.83 | 8 | - | - |
| SMA A=8mm | -0.32 | 10 | - | - |
| SMA A=30mm | 0.02 | 10 | -0.69 | 13 |
| ASCAT | -0.55 | 10 | -0,29 | 13 |
| ESA-CCI | -0,29 | 8 | -0.66 | 11 |
| SMOS | 0.12 | 6 | -0,59 | 6 |
| SMOS-IC | -0.81 | 10 | -0.34 | 13 |
| ERA5 [Daily] | -0.46 | 10 | -0.37 | 13 |
| ERA5 [Hourly] | -0.80 | 10 | -0.63 | 13 |

887

**Table 8: Performance of the SCS-CN model in term of Nash Coefficients for the Rheraya and Issyl events, using the daily or hourly time steps for the different soil moisture products.**

| | | | | Daily | | | | Hourly | |
|---|---|---|---|---|---|---|---|---|---|
| | **ASCAT** | **ESA-CCI** | **SMOS** | **SMOS-IC** | **ERA5** | **In-situ** | **SMA 30mm** | **ERA5** | **In-situ** |
| | | | | | **RHERAYA** | | | | |
| **Min** | -0.15 | - | - | -0.04 | -0.73 | -1.88 | - | -0.01 | 0.15 |
| **Mean** | 0.48 | - | - | 0.58 | 0.45 | 0.25 | - | 0.64 | 0.54 |
| **Median** | 0.57 | - | - | 0.63 | 0.66 | 0.49 | - | 0.73 | 0.61 |
| **Max** | 0.85 | - | - | 0.84 | 0.82 | 0.83 | - | 0.81 | 0.71 |
| | | | | | **ISSYL** | | | | |
| **Min** | - | -56041 | -1938 | - | - | - | -96.08 | -114.60 | - |
| **Mean** | - | -14138 | -324 | - | - | - | -24.77 | -16.74 | - |
| **Median** | - | -254 | -1.80 | - | - | - | -2.46 | -0.85 | - |
| **Max** | - | -2.10 | -0.52 | - | - | - | -0.78 | 0.83 | - |

912     **FIGURES**

913

914
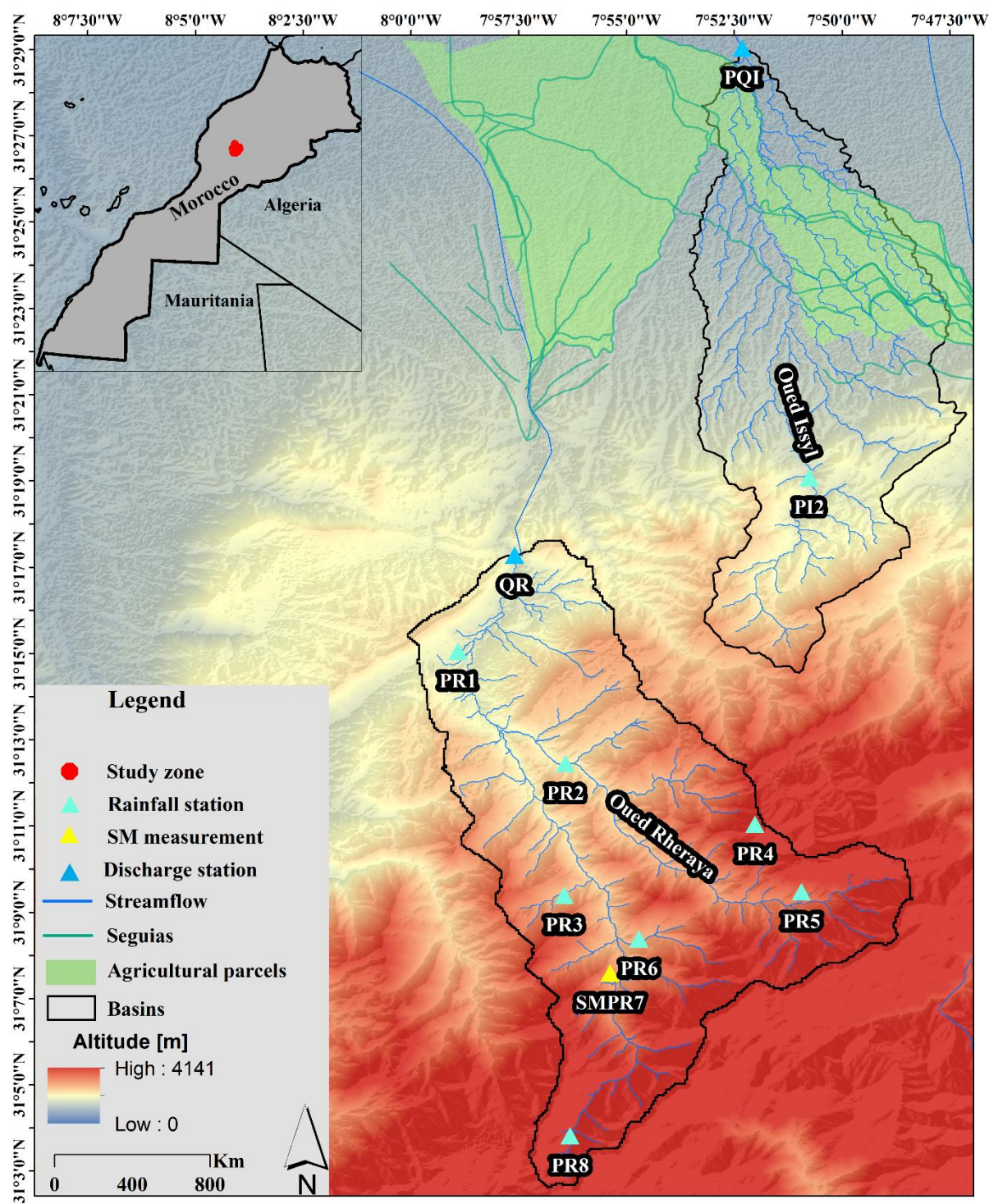
**Figure 1:  Location of Rheraya and Issyl basins, the seguias network, the agricultural parcels and the**
**hydro-meteorological network – PR: Rainfall station in Rheraya, SMPR: Soil moisture measurement+**
**Rainfall station in Rheraya, PQI: Rainfall and discharge station in Issyl, QR: Discharge station in**
**Rheraya.**

919

920
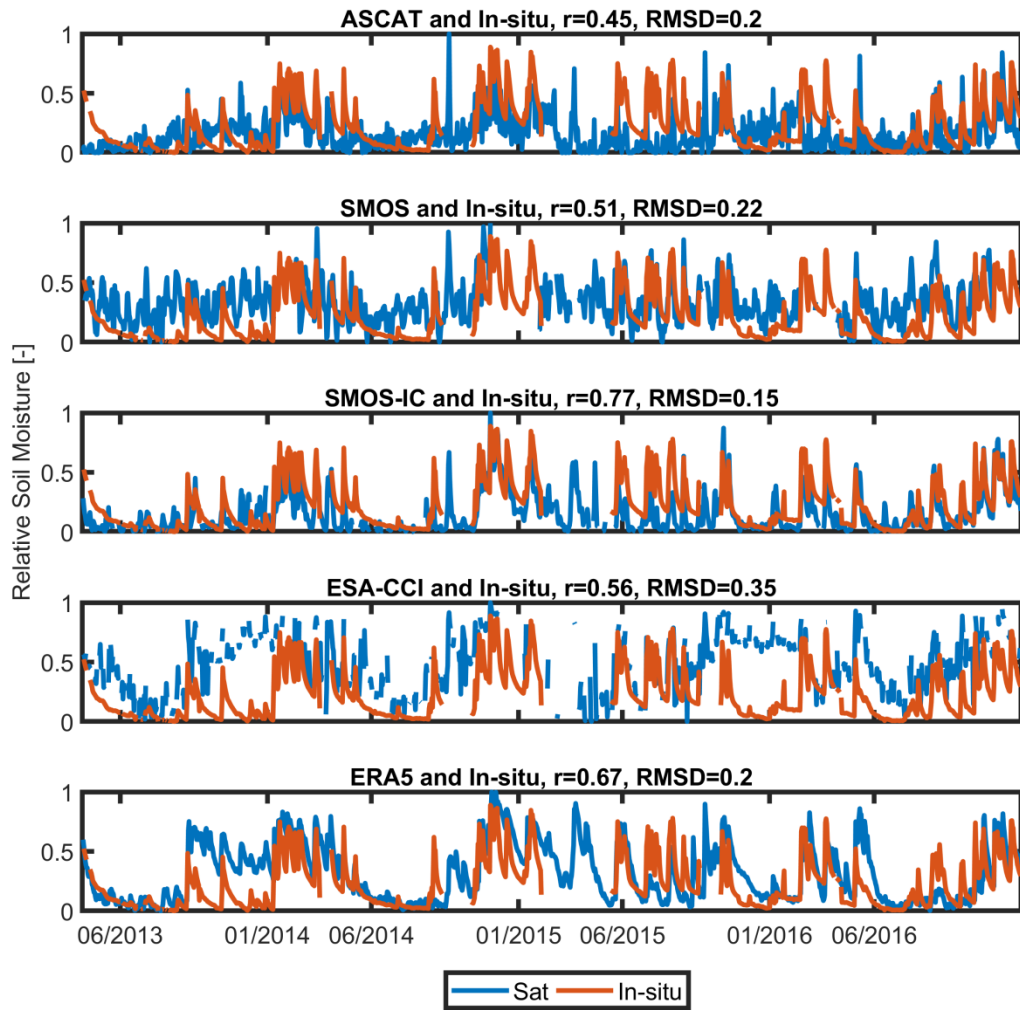
**Figure 2: Comparison between measurements of soil moisture (5cm depth) and different products of soil moisture (Rheraya basin).**
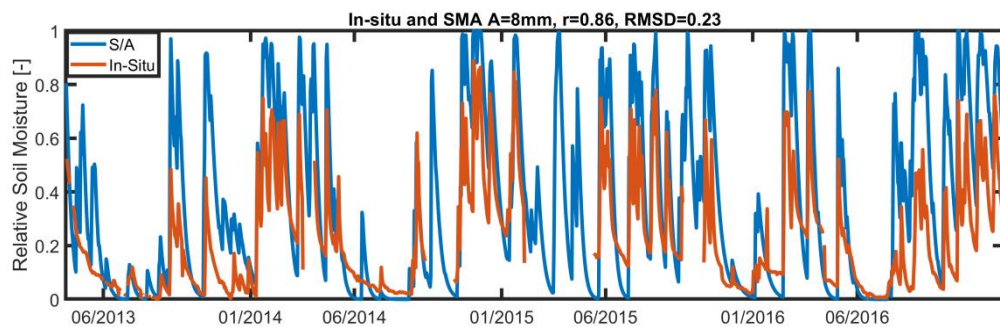
**Figure 3: Relationship between S/A and observed soil moisture data between 08/04/2013 and 31/12/2016 for different values of A (Rheraya basin).**

930
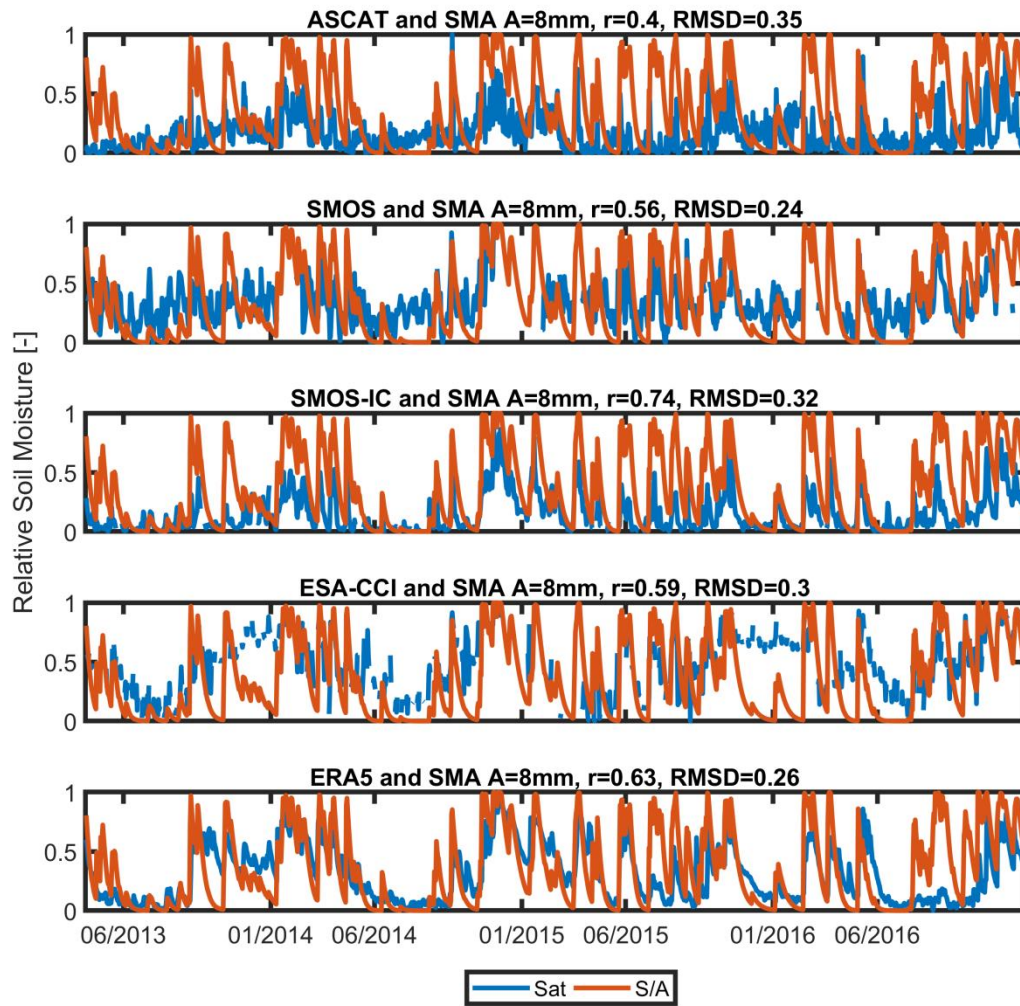
Figure 4: Relationship between the different products of soil moisture and SMA outputs between

08/04/2013 and 31/12/2016 over the Rheraya basin.

933
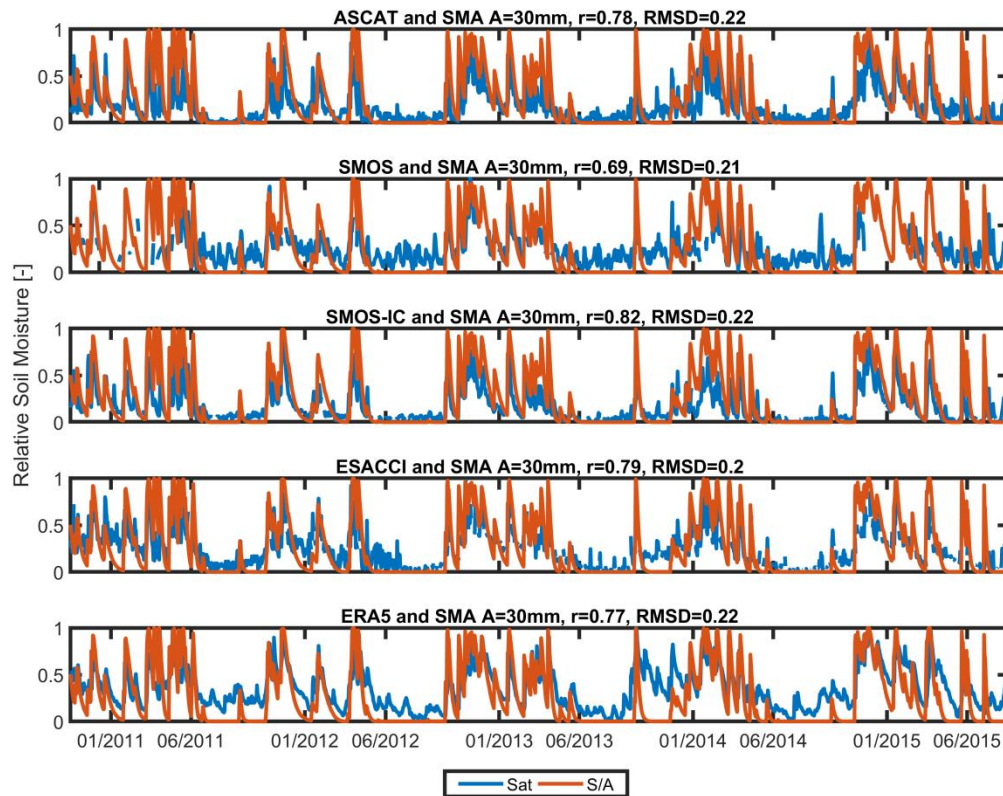
934    Figure 5: Relationship between the different products of soil moisture and SMA outputs

935    between 18/10/2010 and 20/08/2015 in the Issyl basin

936

937
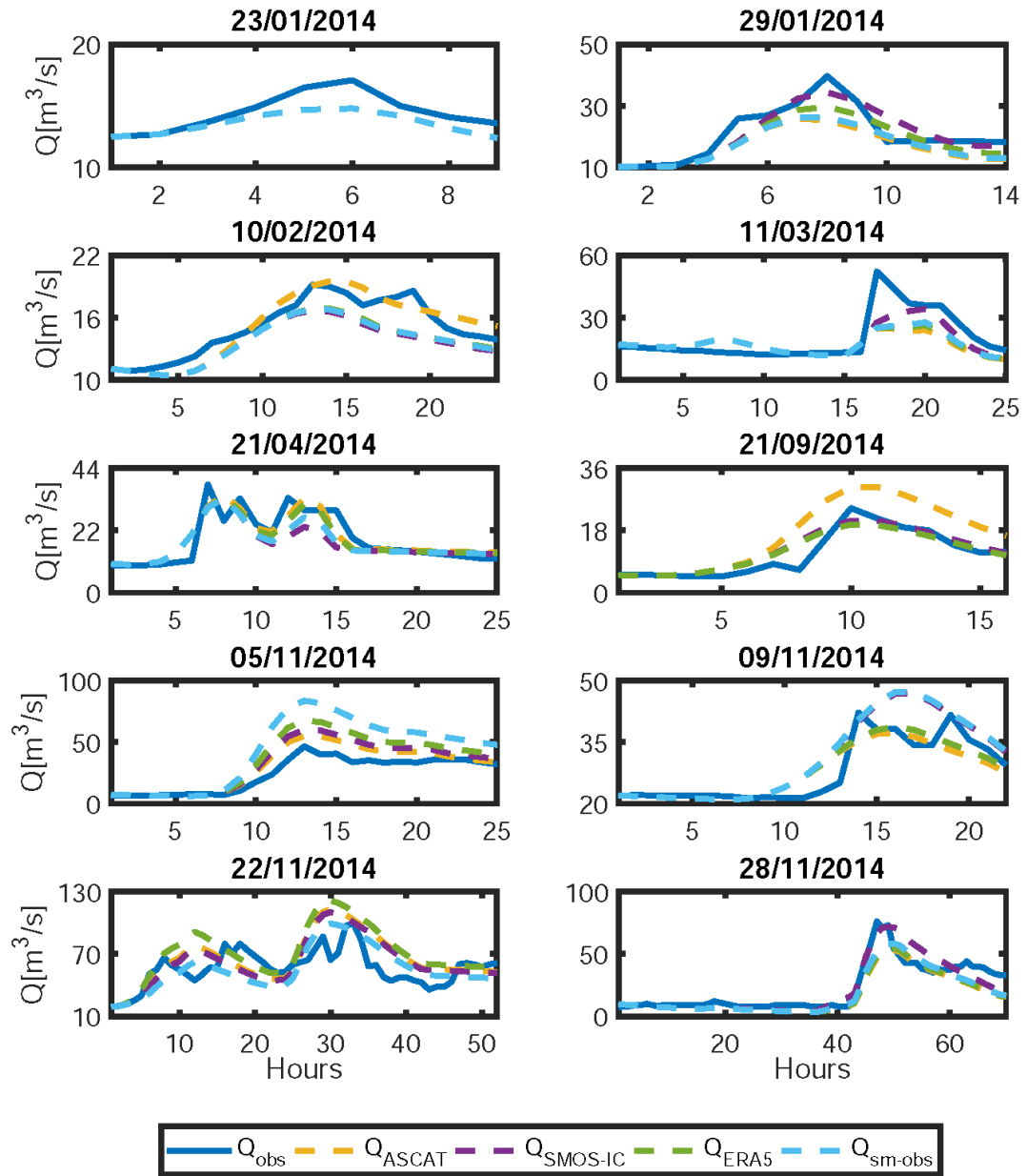
**Figure 6:**

Validation results of flood events simulated for the Rheraya using different soil moisture products with a daily time step: the observed hydrographs ($Q_{obs}$) are compared to the simulated hydrographs using ASCAT ($Q_{ascat}$), SMOS-IC ($Q_{SMOS-IC}$), ERA5 ($Q_{ERA5}$) or observed soil moisture ($Q_{sm-obs}$) to estimate the antecedent soil moisture conditions. The selected flood events are described in Table 2

943

944

945

946

947

948 **Figure 7:**

949 Validation results of flood events simulated for the Rheraya using different soil moisture products with an hourly

950 time step: the observed hydrographs ($Q_{obs}$) are compared to the simulated hydrographs using ERA5 ($Q_{ERA5}$) or

951 observed soil moisture ($Q_{sm-obs}$) to estimate the antecedent soil moisture conditions. The selected flood events are

952 described in Table 2

953

954

955

956
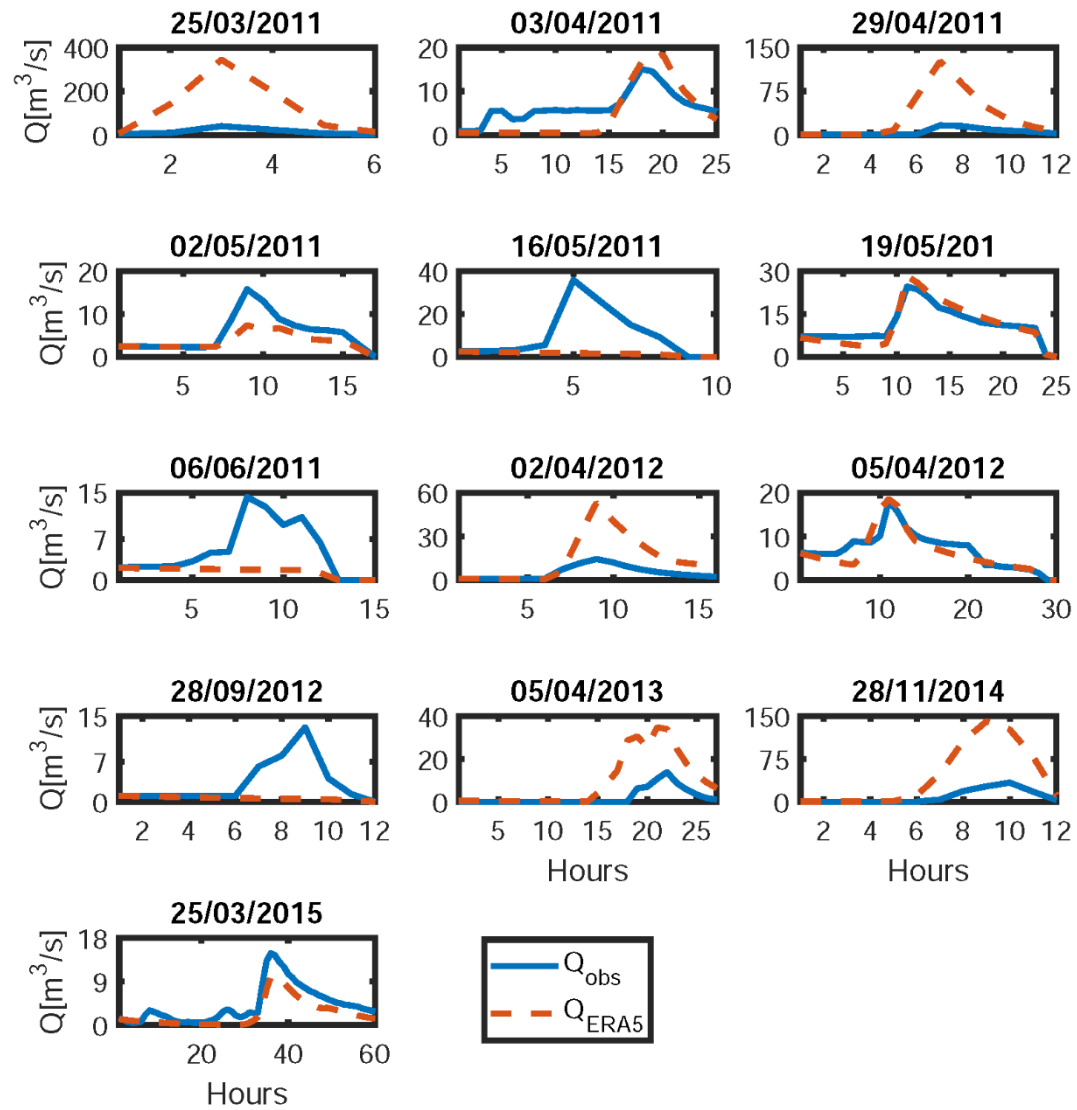
957 **Figure 8:** Validation results of flood events simulated for the Issyl using ERA5 soil moisture at the hourly time step:

958 the observed hydrographs ($Q_{obs}$) are compared to the simulated hydrographs using ERA5 ($Q_{ERA5}$) to estimate the

959 antecedent soil moisture conditions. The selected flood events are described in Table 2

960